Effect of Organic Modifiers on Dynamic and Static Nanomechanical Properties and Crystallinity of Intercalated Clay–Polycaprolactam Nanocomposites

Debashis Sikdar, Dinesh Katti, Kalpana Katti, Bedabibhas Mohanty

Department of Civil Engineering, North Dakota State University, Fargo, North Dakota 58105

Received 31 October 2006; accepted 24 January 2007
DOI 10.1002/app.26284
Published online 2 April 2007 in Wiley InterScience (www.interscience.wiley.com).

ABSTRACT: Polymer clay nanocomposites (PCN) of Polyamide6 and sodium montmorillonite are prepared using different organic modifiers (12-aminolauric acid, *n*-dodecylamine, and 1,12-diaminododecane) to study effect of organic modifiers on structure and nanomechanical properties of PCN. Using X-ray diffraction and differential scanning calorimetry, crystalline nature of PCNs are evaluated. Nanoscale viscoelastic properties of PCNs are evaluated using nanodynamic mechanical analyzer (NanoDMA). Nanoscale elastic modulus and hardness of PCNs are evaluated using nanoindenter. PCNs show enhancement in elastic modulus, storage modulus, loss modulus, and loss factor by maximum amount of 62.88%, 56.38%, 145.74%, and 71.43%, respectively, and decrease in percentage crystallinity by 16.52% compared to pure polymer. This result indicates that organic modifiers have effect on crystallinity and nanomechanical properties of PCN. To evaluate effect of clay loading on nanomechanical properties of PCN, PCN containing 12-aminolauric acid is synthesized with different weight percent (3, 6, and 9% of weight of polymer) of organically modified montmorillonite (OMMT), which shows that nanomechanical properties of PCN improves with increase in clay loading. Our study reveals that change in crystallinity of polymer in PCN may have role in the enhancement of nanomechanical properties of PCNs in comparison to pristine polymer. J Appl Polym Sci 105: 790–802, 2007

Key words: atomic force microscopy (AFM); composites; crystallization; indentation; nanotechnology

INTRODUCTION

Since the development of polymer clay nanocomposites (PCNs) by Toyota R and D labs in 1990 in Japan, PCNs have drawn considerable attention of researchers because of significant improvement in mechanical properties,[1–12] thermal properties,[7,13-20] liquid or gas barrier properties,[4,5,21] etc. in comparison to pristine polymers. Most notable are the improvements in elastic modulus,[4–6] tensile strength or elongation strain,[7,9] and enhancement in thermal resistance and decrease in flammability.[7–12] Because of the significant improvement of properties, PCNs have potential applications in the automobile, aviation, geotextile, biomedical, and other polymer industries where the use of the polymers is abundant and property enhancement (mechanical, thermal, etc) is the primary concern.

In PCN, nanoclay is uniformly dispersed in the polymer matrix. Generally sodium montmorillonite (MMT) is used as clay inclusion due to its highly expansive nature. The MMT is smectite clay mineral that has mica type layered structure where clay sheets are stacked one over another in periodic fashion. The space between two consecutive parallel clay sheets is called interlayer clay gallery. Depending upon the dispersion of nanoclay in the polymer matrix, two types of PCN can be formed: (i) intercalated PCN and (ii) exfoliated PCN. In the intercalated PCN, polymer and organic modifiers enter the interlayer clay gallery by pushing the parallel clay sheets apart by a significant amount while maintaining the periodic crystal structure of MMT clay. On the other hand, when large volume of polymer or modifier enters inside the clay gallery of PCN, the spacing between two parallel sheets becomes so large that clay does not maintain its periodic crystal structure any more. The clay platelets become delaminated in the polymer matrix and form exfoliated PCN.

From literature we have seen that the PCNs show enhanced mechanical, thermal properties; however, the reason behind the property enhancement is not well understood. Unless the mechanisms behind the property enhancement are known, PCN with tailored properties can not be made. The bulk properties

Correspondence to: D. Katti (dinesh.katti@ndsu.edu).
Contract grant sponsor: National Science Foundation; contract grant numbers: MRI 0320657, IMR 0315513.
Contract grant sponsor: National Science Foundation; contract grant numbers: 056020, 0114622.

of nanocomposites largely depend on the microstructure and properties of the constituents at the interfaces.[22] From our steered molecular dynamics prior study[23,24] it appears that inclusion in the interlayer clay gallery has significant influence on the mechanical properties of the clay based nanocomposites. In intercalated PCN, polymer and organic modifiers enter into the interlayer clay gallery of nanosized clay particles. Hence, the properties at the interface of polymer, clay, and organic modifier can be important for the overall properties of PCN. Using nanomechanical experiments (nanoindentation, nanodynamic mechanical analysis, etc.), nanomechanical properties of PCN samples can be found, the results of which may provide some important insight into the effect of nanoscale inclusions and organic modifiers on the properties of nanocomposites. In this study, we have evaluated the dynamic mechanical properties of PCN using nanodynamic mechanical analyzer (NanoDMA), and, its elastic modulus and hardness using nanoindenter.

For the last 100 years, indentation tests have been used to determine the hardness of materials.[25] Here ''hardness'' is the ratio of applied load to the projected contact area of tip probing the sample. In quasi-static nanoindentation test, a controlled load is applied to the sample and corresponding displacement of the indenter is measured. On the basis of well defined models, the load–displacement curve considering the indenter geometry is analyzed for calculating the elastic modulus (E) and hardness (H).[26] Elastic modulus is calculated considering the initial part of unloading curve of load–displacement plot. The viscoelastic properties of polymeric materials are obtained from loss modulus (E'') and storage modulus (E'). The storage and loss moduli are obtained by applying AC force modulation in nanoindentation.[27,28] Recently, some work has been done on the determination of elastic modulus and hardness of PCNs using nanoindentation. Shen et al.[29] studied the nanomechanical properties of PA66 based exfoliated PCN. They reported that for clay loading less than 5 wt %, the nanoclay fillers have dominant role in the creep behavior compared to the reinforcement effect. Beake et al.[30] conducted depth sensing nanoindentation on polyethylene oxide based PCN. According to them, the nanomechanical behavior of PCN largely depends on the method of synthesis and clay loading in PCN. Shen et al.[31] studied the effect of strain rate on PA66 based exfoliated PCN. At different strain rates, surface of PCN and PA66 were indented, which showed significant strain rate hardening in PCNs; however, almost no effect of strain rate was observed on elastic modulus of PCN. In a separate study[32] they studied the same PA66 sample prepared by injection molding to evaluate the effect of clay platelet orientation on the elastic modulus in nanoscale. They observed that uneven distribution of clay fillers and crystallinity of polymeric materials contributes to the enhancement of elastic property of PCN. For PA6 based PCN, they further showed that hardness and elastic modulus of PCN vary depending on the crystalline nature (α and γ forms) of polymer. The elastic modulus for PCN having γ-crystalline PA6 was found to be 53% lower than that of PCN containing α-crystalline polymer.[33] Hu et al.[34] used a nanoindentation technique to evaluate the elastic modulus of nylon11 based PCN, which was found to be 27% higher than that of pristine nylon11. Nai et al.[35] studied the creep behavior of PA6 based PCN using nanoindentation for different loading rates and holding period of loads. Beake et al.[36] studied the behavior of rubber-modified acrylonitrile butadiene styrene (ABS) based PCN against repetitive loading. Bhaskar et al.[37] studied the stress–strain behavior of poly (methyl methacrylate) based PCN using nanoindentation.

Although studies have been conducted for evaluating viscoelastic properties of PCN in the macro scale using thermal gravimetric analyzer,[38–49] little work has been done for evaluating the viscoelastic properties of pure polymeric materials at nanometer length scale. Recently, dynamic nanoindentation test[50] has been performed on ultra high molecular weight polyethylene at nanoscale using dynamic nanoindentation, in which they found that the improvement of storage and loss modulus depends on the method of crosslinking of polymer. Asif et al.[51] and Hayes et al.[52] studied the viscoelastic properties of epoxy resin with dynamic nanoindentation. However, in literature, no NanoDMA studies have been reported so far on other polymeric materials or PCN. Recently, Mohanty et al.[53] using dynamic nanoindentation experiment reported that nacre containing mostly aragonite shows viscoelastic behavior due to the presence of protein sandwiched between two aragonite layers. For the first time, in the current study, we have evaluated the viscoelastic response of PCN using dynamic nanoindentation. Experiments are conducted using a load of 10,000 μN at a frequency of 50 Hz. To investigate the role of organic modifiers on viscoelastic properties of PCN, the tests are performed on PA6 based PCN using three different organic modifiers.

Ma et al.[11] in their work have showed that using different organic modifiers, different bulk mechanical and thermal properties of PCN are obtained. This clearly indicates that in addition to enhancement of miscibility of hydrophobic polymer with clay, organic modifier has some definite contribution to the property enhancement of PCN. Hence in this work, we have synthesized the PCNs containing polyamide 6, MMT, and three different organic modifiers: 12-aminolauric acid, *n*-dodecylamine, and 1,12-diamino-

dodecane, and evaluated their dynamic mechanical property, elastic modulus, and hardness in the nanometer length scale to evaluate the effect of organic modifiers on the nanomechanical properties of PCN. To observe the effect of clay loading on mechanical properties of PCN, same polymer and organic modifier (12-aminolauric acid) containing three different clay loading (3, 6, and 9 wt % of 12-aminolauric acid based OMMT of the weight of polymer) are synthesized and their nanomechanical properties are evaluated in this work. X-ray diffraction (XRD)[54–65] and differential scanning calorimetry (DSC)[66–76] are often used techniques to study the crystallinity of polymeric materials. In this work, the crystallinity of PCN is studied using XRD and DSC to evaluate the change in crystallinity of PCN with respect to pristine polymer and its effect on nanoscale property enhancement of PCN.

MATERIALS AND METHODS

Materials

The three organic modifiers 12-aminolauric acid [$NH_2(CH_2)_{11}COOH$], *n*-dodecylamine [$NH_2(CH_2)_{11}CH_3$], and 1,12-diaminododecane [$NH_2(CH_2)_{12}NH_2$] are obtained from TCI America. Na-MMT (Swy-2, Crook County, Wyoming, USA) of cationic exchange capacity 76.4 mequiv/100 mg is supplied by the Clay Minerals Repository at the University of Missouri, Columbia, MO, USA. Polyamide6 (PA6) $[(CH_2)_5CONH]_n$ of molecular weight 16,000 is purchased from Polysciences (USA). Methanol anhydrous (99.9%), formic acid (FA) (97%), silver nitrate, acculute standard volumetric solution, final concentration 0.1*N*, and 0.1*N* hydrochloric acid [HCl] are purchased from Alfa Aesar, MA, USA.

Na-MMT is most commonly used clay for making PCN due to its highly expansive nature, which allows formation of nanosized inclusions either through intercalation or exfoliation. Hence in this work, MMT is used as clay for synthesizing PCN. PA6 is a common type of hydrophobic polymer, which has wide range of industrial applications. Mechanical and thermal properties of this polymer in PCN have been studied extensively by researchers making PA6 a good candidate as a model system for further research on PCN where understanding key mechanisms for property enhancement is the goal.

Preparation of organically modified montmorillonite (OMMT)

The synthesis of OMMT is done following the procedure described in our earlier work.[77] Three different organic modifiers, 12-aminolauric acid, *n*-dodecylamine, and 1,12-diamonidodecane, are used for synthesis of three different OMMTs in the current work, which have been named in this paper as OMMT-lauric, OMMT-dodecyl, and OMMT-dodecane respectively. The dried OMMT is ground and sieved through a 45 μm sieve for synthesis of PCN.

Synthesis of polymer clay nanocomposites (PCN)

For the synthesis of PCN, 10 g of PA6 is added to 155.73 mL (190 g) of FA and stirred vigorously for 40 min to make a uniform solution. PCNs containing three different OMMTs, OMMT-lauric, OMMT-dodecyl, and OMMT-dodecane, are synthesized, which are named as PCN-lauric, PCN-dodecyl, and PCN-dodecane, respectively, in this work. For processing of 9% PCN, 0.9 g of OMMT is uniformly dispersed in the PA6-FA solution and stirred vigorously for 6 h at room temperature. In the resulting solution, DI water is added and fibrous PCN is formed. The fibrous PCN is washed repeatedly in DI water until it is free from FA. Then the PCN is washed several times with methanol to remove water from PCN. Finally it is placed in the vacuum oven at 40°C for 24 h to remove methanol and fibrous PCN is obtained. Three types of PCN containing 9 wt % of OMMT loading of the weight of polymer are synthesized. Additionally, for PCN-lauric, 3 and 6 wt % PCNs (containing OMMT @ 3 and 6 wt % of the weight of polymer) are synthesized following identical synthesis route.

Sample preparation of PCN for XRD, DSC, Nanoindentation, and NanoDMA

The fibrous PCN sample is pressed under a pressure of 80 MPa for a duration of 10 min to form lamellar sheet of PCN of thickness 0.80 mm and is used for XRD. For DSC, nanoindentation, and NanoDMA experiments, 4 g of fibrous PCN is placed in a cylindrical mold of diameter 12.7 mm fitted with a plunger. The mold containing PCN sample is gradually heated under vacuum to 230°C. The temperature is raised from room temperature to 200°C in 1 h at 50°C steps. The temperature is further raised to 230°C in two equal steps of duration of 30 min per step. After melting, the PCN samples are pressed under a pressure of 1 MPa for duration of 1 min and quenched to room temperature under atmospheric condition. The solid cylindrical sample of PCN having diameter of 12.7 mm is formed. The sample is cut into circular pieces of average thickness of 1 mm for using in nanoindentation and NanoDMA experiments. For DSC, the pieces of sample of average weight 10 mg are used. PA6 sample was also subjected to the same conditions used in the synthesis of PCN.

The AFM phase image of solid PCN sample is shown in Figure 1. From the phase image, the phase

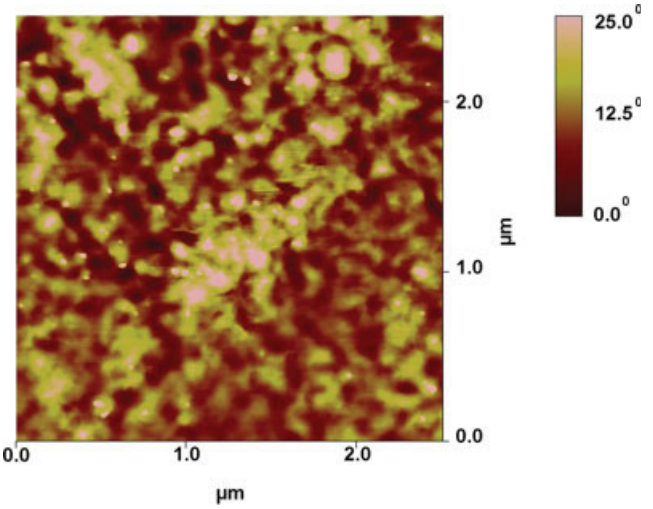

Figure 1 AFM image showing the different phases of PCN: OMMT (lighter spots) are uniformly dispersed in polymer matrix (darker spots). [Color figure can be viewed in the online issue, which is available at www.interscience.wiley.com.]

lag of dynamic amplitude of different constituents present in the composite are obtained. Thus from phase image, the pattern of dispersion and size of different phases present in the composites can be obtained. In the phase image of PCN, the lighter spots and darker spots correspond to the clay reinforcement and polymer matrix, respectively. Here the polymer is more viscoelastic as compared to clay particles and thus shows as a darker contrast in the phase image. Our observation agrees with the observation of Scott and Bhushan[78] where the PET is more viscoelastic than the embedded ceramic particles and thus PET has darker contrast in the phase image. From Figure 1, it is evident that the clay platelets are uniformly dispersed in the polymer matrix of PCN.

Characterization

X-ray diffraction (XRD)

The XRD of PCNs is done using X-ray diffractometer (model Philips X'pert, Almelo, Netherlands). The X-ray diffractometer is equipped with secondary monochromator and Cu-tube. Cu Kα radiation of wavelength 1.54056 Å is used in the experiment. The wide angle XRD of PCN samples are done at a scan rate of 3°/min and for scan range of $2\theta = 2.01°$–60°. The results obtained from XRD are used for analysis of *d*-spacing and crystallinity of PCN.

Differential scanning calorimetry (DSC)

DSC experiments are conducted using differential scanning calorimeter (model Q1000 DSC) of TA instruments (New Castle, Delaware). In the experiment, the sample is first heated from 30 to 100°C in 3 min and then the temperature is stabilized at 100°C for 10 min. The temperature is further increased to 250°C at a heating rate of 10°C/min and is stabilized at 250°C for 10 min. Then the sample is cooled down from 250 to 30°C at the rate of −10°C/min. In the final heating cycle, the sample is further heated from 30 to 250°C at a rate of 20°C/min. The results obtained from DSC are used for determination of crystallinity at melting of PCN using the following equation:[79]

$$\%\,\text{crystallinity} = 100 \times (\Delta H_m)/(\Delta H_{\text{lit}})$$

where, ΔH_m is the enthalpy of melting of sample, and ΔH_{lit} is the enthalpy of melting for 100% crystalline material, the value of which for PA6 is 203.06 J/g.[67]

Nanoindentation

Nanoindentation tests on PCN are performed using a Triboscope nanomechanical testing instrument (Hysitron, MN, USA). The triboscope is operated with a multimode atomic force microscope (AFM) (Veeco Metrology Group, Santa Barbara, CA, USA). A trigonal pyramid shaped diamond Berkovich tip is used for the experiments. All the tests are performed at room temperature and pressure in a direction perpendicular to the face of the PCN. A 5-5-5 trapezoidal loading function is used in the quasi-static (load controlled) nanoindentation test. In the loading function, the first segment indicates that time for reaching maximum load of indentation is 5 s. The second segment indicates the hold period of peak load, which is 5 s in this case. The last segment indicates the unloading time from peak load to zero load, which is set in the experiment as 5 s. Contact mode atomic force microscopy using Multimode AFM having a Nnaoscope-IIIa controller equipped with a J-type piezo scanner (Veeco Metrology Group) is used for imaging the PCN samples. The contact mode AFM image is generated using silicon nitride tips from Veeco.

The solid PCN sample is prepared as described in a previous section and is cut using a diamond-wafering blade (Buehler, Isomet) and care is taken to obtain a flat surface for the indentation tests. The tests are performed at a load of 10,000 μN and 21 indentations are done at that load on each sample.

Using the Oliver-Pharr method,[25] the elastic modulus (E) and hardness (H) are determined from the load–displacement curves. In this method, the unloading segment of the curve is fitted to a power-law function to obtain the contact depth. Using the initial straight line portion of the unloading curve and differentiating the power-law function the stiffness ($S = dP/dh$) is calculated. The reduced elastic modulus (E_r) of PCN is obtained using a relation involving

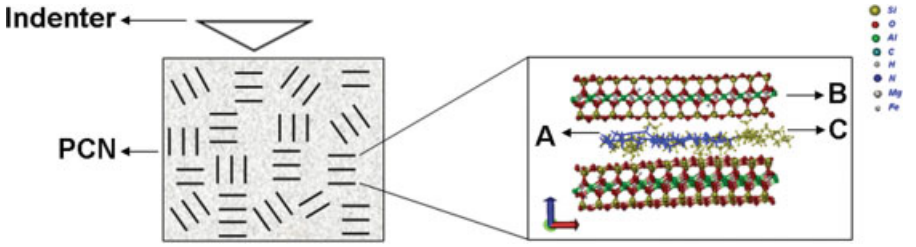

Figure 2 Schematic diagram showing the indentation on PCN. The inset shows the molecular model of intercalated PCN. (A), (B), and (C) represent MMT clay sheet, polymer, and organic modifier, respectively, in the intercalated PCN. [Color figure can be viewed in the online issue, which is available at www.interscience.wiley.com.]

contact stiffness and the contact area. As the sample and indenter, both undergo elastic deformation, the deformations of both of them are considered in calculating reduced elastic modulus (E_r) of sample. The reduced elastic modulus is calculated as follows:

$$1/E_r = \left(1 - \nu^2\right)/E + \left(1 - \nu_i^2\right)/E_i$$

where E and ν are the elastic modulus and poison's ratio of the sample, respectively; and E_i and ν_i are the respective properties for the indenter. For diamond $E_i = 1141$ GPa and $\nu_i = 0.07$.

Indentation hardness is defined as the mean pressure the material will support under load. The hardness is calculated by dividing the maximum load by the contact area of the indenter at peak load.

$$H = P_{\max}/A$$

where, H is hardness, $P_{\max}$ is the maximum load experienced by sample, and A is the contact area at peak load.

Nanodynamic mechanical analysis (NanoDMA)

Dynamic nanoindentation tests on PCN are performed using a Triboscope nanomechanical testing instrument (Hysitron). The triboscope is operated with the multimode AFM (Veeco Metrology Group). The load resolution of triboscope is 1 nN and displacement resolution is 1 nm. A trigonal pyramid shaped diamond Berkovich is used in the experiment. All the tests are performed in room temperature and pressure in a direction perpendicular to the face of the PCN as shown in Figure 2.

In the variable dynamic load test on PCN, the load and load–amplitude are changed maintaining a constant frequency. The load range is chosen to get the property from the clay–polymer interfaces in PCN, which are 5000 and 10,000 μN as the beginning and end loads, respectively. The peak load from starting load point is reached in 11 segment steps at a loading rate of 1000 μN per second. The starting dynamic load is 50 μN and the frequency of loading function is 50 Hz.

During the dynamic nanoindentation test, the displacement amplitude, load amplitude, and phase lag are measured to calculate the storage modulus, loss modulus, and loss factor (tanδ) of PCN samples. The instrument and sample to be tested are modeled by damped harmonic oscillator with single degree of freedom.[80] A small oscillatory load (P) with a known load amplitude (P_0) and frequency (ω) is applied on the sample in the dynamic nanoindentation test. Using lock-in amplifier, the alternating displacement response during the experiment is measured at the same testing frequency. The sinusoidal behavior of the load (P) and the resulting displacement is given by the following expression:

$$P = P_0 \sin \omega t$$

$$X = X_0 + \sin(\omega t - \varphi)$$

Here, t is the time and ϕ is the phase difference between load amplitude (P_0) and displacement amplitude (X_0).

The stiffness and the damping coefficient observed in dynamic nanoindentation test is a combined response of the instrument and the specimen under testing. Hence, the response of the instrument must be isolated from the gross response for obtaining the true dynamic properties of sample. Therefore, prior to the experiment, the damping coefficient (C_i), stiffness (k_0), and mass (m) of the indenter are obtained by air calibration. This is followed by real-time correction of the aggregate response for the response of the instrument. The portion of material's displacement response that is in-phase with the oscillating load gives the elastic response of the material. The energy that is absorbed by the material during the contact with indenter gives the viscoelastic response of the sample. It is produced by the out-of-phase portion of response. The values of storage modulus (E'), loss modulus (E''), and loss factor (tanδ) are given by the following expressions:

$$E' = \frac{k_s\sqrt{\pi}}{2\sqrt{A_c}}$$

$$E'' = \frac{\omega C_s \sqrt{\pi}}{2\sqrt{A_c}}$$

$$\tan\delta = \frac{\omega C_s}{k_s}$$

where, k_s and C_s are the stiffness and damping coefficient of the specimen, respectively, and A_c is the projected contact area of indenter on the surface of specimen.

RESULTS AND DISCUSSION

X-ray Diffraction (XRD)

The XRD plot of PCNs containing 9 wt % of OMMT and polymer is shown in the Figure 3. The low angle peaks are observed at $2\theta = 6.54^\circ$, 6.60°, and 6.66° in PCN-lauric, PCN-dodecyl, and PCN-dodecane, respectively, which correspond to the d_{001} peak of intercalated PCNs. The corresponding d-spacing of PCN-lauric, PCN-dodecyl, and PCN-dodecane are found to be 13.51, 13.39, and 13.27 Å, respectively. However, this low angle peak is not found in pure PA6. The presence of low angle ($< 10^\circ$) XRD peak in PCNs is an indication of the presence of intercalated OMMT in PCN.

PA6 is a highly crystalline polymer, which shows polymorphism containing α-monoclinic, γ-monoclinic, and amorphous phase in its structure. The α and γ crystalline phases in PA6 are observed in the range of $2\theta = 19^\circ48'$–$24^\circ3'$.[81] The α form has zigzag planar conformation, which is formed by anti parallel chains connected by hydrogen bonds. The γ form is composed of parallel chains connected by hydrogen bonds. The α crystalline phase is thermodynamically more stable in comparison to γ crystalline form.[11] The XRD peaks in specified range of $2\theta = 19^\circ48'$–$24^\circ3'$ are deconvoluted as shown in Figure 4 to measure the α and γ crystalline phases of PCNs and pure PA6. Peaks 1, Peak 2, and Peak3 in Figure 4 represent the α_1-monoclinic, γ_2-monoclinic, and α_2-monoclinic crystalline phases of PA6, respectively,.[81] The peak positions corresponding to these crystalline phases are shown in Table I. For the assessment of relative proportion of α and γ crystalline phases in PCNs and PA6, the area under the peaks of different crystalline phases and their ratios are calculated from Figure 4, which are presented in Table II. Column 5 in Table II gives the ratio of α and γ crystalline phases in PCNs and PA6. It is observed that the PCN-lauric-9% and PCN-dodecyl-9% have predominantly γ crystalline phase. On the other hand, PA6 has dominantly α crystalline phase. This phenomenon agrees with the previous observation.[82] However, in PCN-dodecane-9%, the crystalline phase is more close to pure PA6 where the α crystalline phase is dominantly observed. The nanoclay fillers in PCN disrupt the ordered lamellar stacking of polymer chain, which results in the transformation of crystallinity from α phase in PA6 into γ phase in PCN. The PCN-dodecane contains 1,12-diaminododecane, which has two protonated amine groups at both the ends of each modifier molecules. Protonated amine groups of intercalated modifiers have relatively stronger interactions with the interlayer clay surface in comparison to the end functional groups of other two modifiers. Hence in PCN-dodecane, the intercalated organic modifiers have relatively feeble interactions with intercalated polymer. The relatively weaker interaction may not be able to disrupt the ordered lamella stacking of polymer and thus crystalline phase in PCN-dodecane is found more close to pure PA6, which is dominantly α crystalline in nature.

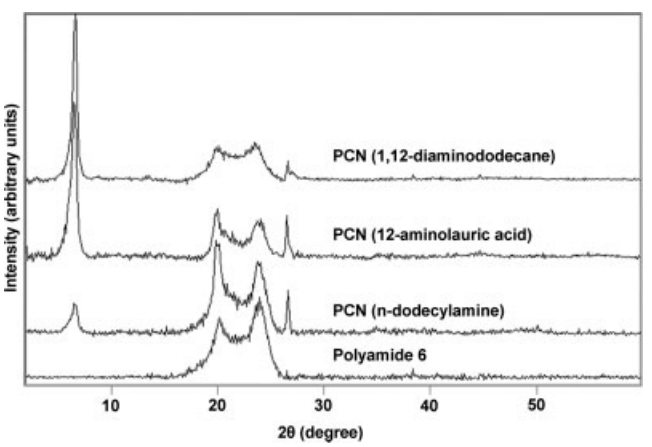

Figure 3 XRD characteristics of pure polymer, PA6, and PA6 based PCNs.

Differential Scanning Calorimetry (DSC)

Melt crystallization experiments are conducted on pure PA6 and PA6 based PCNs containing different organic modifiers to assess their effect on the crystallization behavior of PCNs. The heat of fusion and the percent of melt crystallization of different PCNs containing 9 wt % of OMMT are shown in Table III. From the results in Table III, it is observed that pure PA6 shows relatively higher crystallinity than that of PCNs. Pure PA6 has orderly oriented lamellar stacks that impart crystallinity. In PCN, when polymer chains are intercalated into clay sheets, the nanoclay fillers appear to disrupt the regular ordered orientation of polymer, which results in the reduction of crystallinity of PCN.

All PCNs are synthesized with 9 wt % of OMMT containing identical polymer and clay, however, with different organic modifiers. Although the PCNs contain the same clay loading, it is observed from Table III that PCNs containing different types of

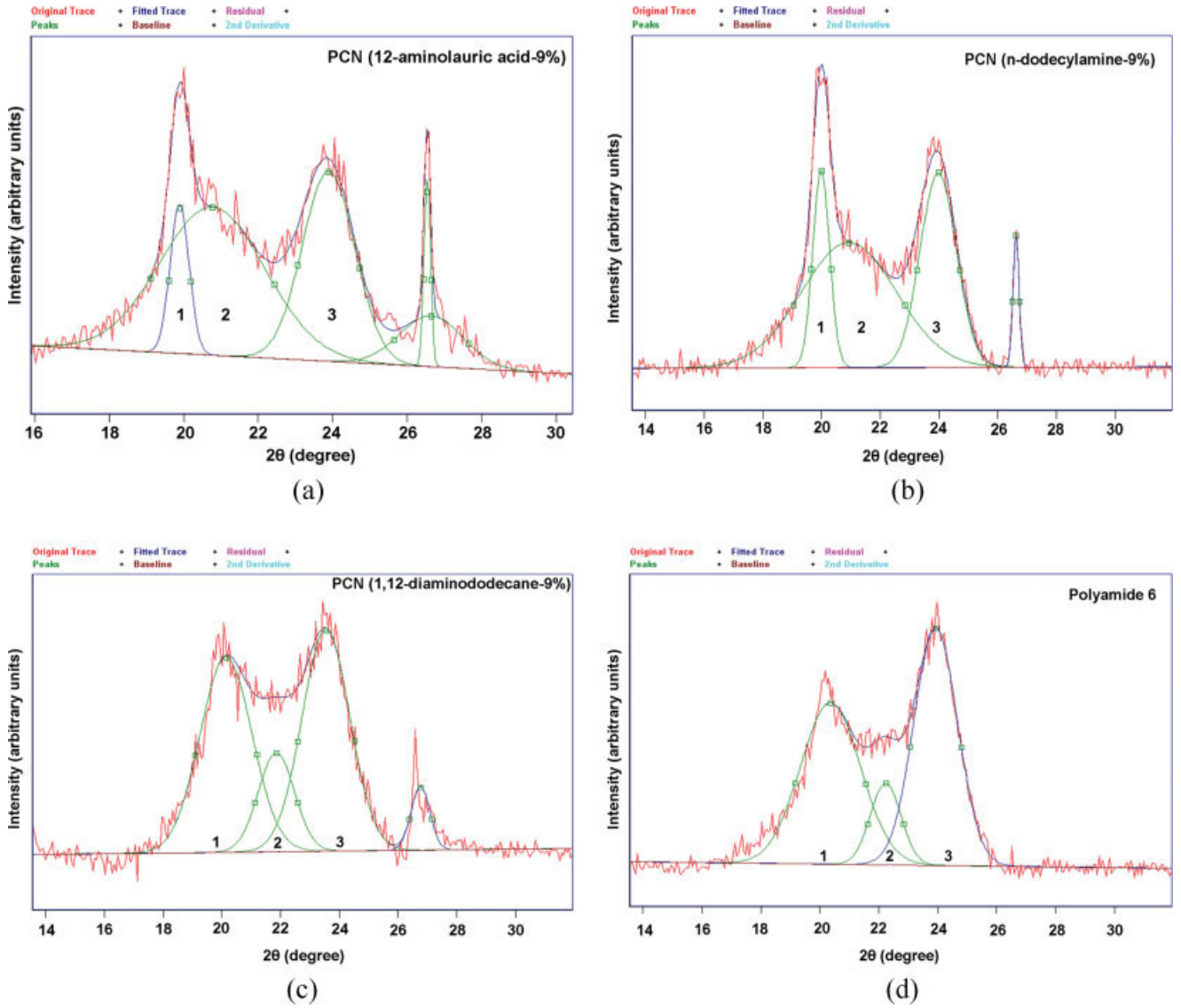

Figure 4 Deconvoluted XRD peaks showing α and γ crystalline phases of polymer of (a) PCN-lauric-9 wt %, (b) PCN-dodecyl-9 wt %, (c) PCN-dodecane-9 wt %, and (d) pure PA6. [Color figure can be viewed in the online issue, which is available at www.interscience.wiley.com.]

organic modifiers show different amounts of crystallinity. This phenomenon leads to the conclusion that organic modifiers have a significant impact on the crystallinity of PCN.

In our previous photoacoustic Fourier transform infrared spectroscopy (PA-FTIR) and molecular dynamics (MD) studies,[77,83] it is observed that there are only nonbonded interactions between the constituents of PCN. From MD study,[84] in PCN-lauric-9%, the strongest attractive interaction is observed between clay and organic modifier followed by the interactions between clay and polymer, and polymer and organic modifier. The three modifiers investigated have almost same backbone-chain length; however, the end functional groups of the modifiers vary from each other as shown in Table IV. Thus different amounts of interactions are due to end functional groups between the constituents of the PCNs. The difference in interactions in PCN due to different modifiers may be responsible for the different amounts of crystallinity in PCNs. In the PCN-lauric-9%, the polymer (PA6) structure appears most disturbed by the interactions of the modifier resulting

TABLE I
Position of XRD Peaks Corresponding to α and γ Crystalline Phases of PCNs and Pure Polymer

Sample	Center of Peak-1 (2θ)	Center of Peak-2 (2θ)	Center of Peak-3 (2θ)
PCN-lauric-9%	19°53′	20°46′	23°53′
PCN-dodecyl-9%	19°59′	20°56′	23°59′
PCN-dodecane-9%	20°8′	21°51′	23°33′
Pure PA6	20°22′	22°14′	23°56′

TABLE II
Area of Deconvoluted XRD Peaks of α and γ Crystalline Phases of PCNs and Pure Polymer

Sample (col. 1)	Area of Peak-1 (col. 2)	Area of Peak-2 (col. 3)	Area of Peak-3 (col. 4)	(col.2 + col. 4)/(col. 3) (col. 5)
PCN-lauric-9%	84.31	465.12	298.21	0.82
PCN-dodecyl-9%	209.46	740.51	441.38	0.88
PCN-dodecane-9%	567.15	200.86	593.91	5.78
Pure PA6	746.97	192.33	801.71	8.05

in the lowest crystallinity followed by PCN-dodecyl-9% among the three PCNs. It appears that in PCN-dodecane-9%, polymer structure may be least influenced by organic modifier and thus resulting in the highest crystallinity among all the PCNs. Pure polymer has the highest crystallinity.

These differences in crystallinity of PCNs may be attributed to nanoscale clay inclusions and the interactions between its constituents. It appears that the inclusions and the interactions inhibit the formation of periodic structure of the polymer resulting in the low crystallinity. For the same amount of nanoscale inclusions and for different organic modifiers, the difference in crystallinity may be attributed to the differences in interactions between the constituents. It is likely that higher interactions between the constituents may result in fewer formation of periodic structure resulting in lower crystallinity.

To assess the effect of clay loading on the crystallization behavior of PCN, the PCN-lauric with three different OMMT loading (3, 6, 9% of the wt of polymer) are tested for melt crystallization, and the results are presented in Table V. It is observed that with increase of clay loading in PCN, more polymer chain will be intercalated in the interlayer clay gallery. Thus it appears that greater amount of ordered lamellar conformations of polymer is disrupted resulting in the reduction of crystallinity of PCN with the increase in clay loading.

Nanoindentation

Effect of organic modifier on elastic modulus and hardness of PCN

To evaluate the effect of organic modifier on nanomechanical properties of PCN, nanoindentation experiments are conducted on PCN samples containing different organic modifiers. The results are presented in Table VI. It is observed that the hardness of PCN is higher than that of pure PA6, whereas no significant change is observed in PCNs containing the three different modifiers that ranges between 0.165 and 0.171 GPa. The depth of penetration of indenter tip of all three PCNs is very similar (in the range 1619–1629 nm) under the maximum loading of 10,000 μN. This results in approximately the same area of contact as shown in eq. (2) of a previous section.

The elastic moduli of PCNs containing three different organic modifiers with 9% OMMT loading are plotted as shown in Figure 5. It is observed that the elastic modulus of all PCNs is higher than that of pure PA6 ($E = 3.352 \pm 0.169$ GPa). Among PCNs, PCN-lauric has the highest elastic modulus with a value of 5.460 ± 0.267 GPa followed by PCN-dodecyl with value of 4.766 ± 0.108 GPa. The PCN-dodecane has the least elastic modulus among the PCNs with a value of 4.417 ± 0.010 GPa.

Hence from the results it is seen that the PCNs containing same polymer, PA6 and clay but with different organic modifiers have different values of elastic modulus at nanometer length scale. This indicates that organic modifiers have significant influence on the elastic modulus of PCN. From DSC result we have seen that crystallinity of PCNs decreases in the order of PCN-dodecane, PCN-dodecyl, and PCN-lauric. The values of elastic modulus decrease in the reverse order, i.e., in the sequence of PCN-lauric, PCN-dodecyl, and PCN-dodecane. Thus from the nanoindentation tests, it is observed that crystallinity decreases with increase in elastic modulus of PCN. It appears that organic modifiers have significant influence on the elastic modulus of PCNs. The different organic modifiers due to different end functional groups may have resulted in different

TABLE III
Change of Crystallinity in PCNs of 9% OMMT Loading with Varying Organic Modifiers

Sample (col. 1)	ΔH_m (J/g)	% Crystallinity
PCN-lauric-9%	46.81	23.05
PCN-dodecyl-9%	50.18	24.71
PCN-dodecane-9%	51.82	25.52
Pure PA6	56.06	27.61

TABLE IV
Dynamic Mechanical Properties of PCN-Lauric with Different OMMT Loading

Organic modifier	Methylene chain	End groups
12-Aminolauric acid	$(CH_2)11$	NH_3, COOH
n-Dodecylamine	$(CH_2)11$	NH_3, CH_3
1,12-Diaminododecane	$(CH_2)12$	NH_3, NH_3

TABLE V
Change of Crystallinity in PCN-Lauric with Varying OMMT Loading

Sample, (col. 1)	ΔH_m (J/g)	% Crystallinity
PCN-lauric-9%	46.81	23.05
PCN-lauric-6%	53.26	26.23
PCN-lauric-3%	53.63	26.41
Pure PA6	56.06	27.61

amounts of crystallinity in PCNs. The different amount of crystallinity produce different amount of entanglement of polymer chain with other constituents of PCN and thus resulting in the different nonbonded interactions of interphases in PCNs. Properties of composites largely depend on the microstructure and interfacial interactions of the constituents of composites. Hence the different amount of crystallinity caused by different organic modifiers resulting in the different structure and interfacial interactions in PCN may be attributed to the differences in elastic modulus of PCN. The higher the crystallinity, the lower the entanglement of polymer chains with other constituents of PCN, which may result in lesser interactions between the interphases of PCN resulting in lesser elastic modulus.

Effect of clay loading rate on elastic modulus and hardness of PCN

To evaluate the effect of clay loading on elastic modulus and hardness of PCN, PCN-lauric with 3, 6, and 9 wt % of OMMT loading are tested with quasi-static nanoindentation experiments. The result of OMMT loading amount on elastic modulus of PCN as presented in Table VII are graphically plotted in Figure 6. From Figure 6, it is observed that with increase in clay loading from 3 to 9 wt %, elastic modulus of PCN increases from 4.43 to 5.46 GPa, which corroborates the DSC results. As seen from DSC results, with the increase of clay loading, the crystallinity of intercalated polymer decreases. It appears that the increase in disorderliness of intercalated polymer structure increases the entanglement of polymer with the amount/percent of clay and modifier in PCN and results in higher interfacial interactions of polymer with the other constituents

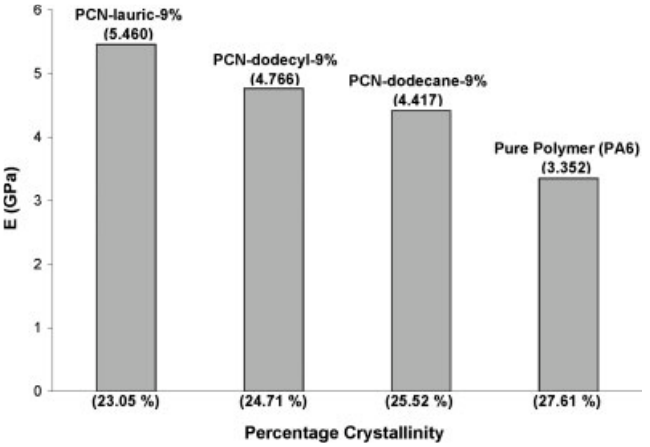

Figure 5 Effect of organic modifiers on elastic modulus of PA6 based PCNs.

of PCN. The nanoclay fillers act as reinforcing agent in PCN, with the interlayer having high elastic modulus of 25–30 GPa.[24] Thus, with the increase of clay loading, in addition to the increase of interfacial interaction of polymer, the reinforcing property of nanoclay itself may contribute to the enhancement of elastic modulus of PCN.

Nanodynamic mechanical properties of PCN

Effect of organic modifiers on nanodynamic mechanical property of PCN

The dynamic nanoindentation tests on the PA6 based PCN containing three different organic modifiers of 12-aminolauric acid, *n*-dodecylamine, and 1,12-diaminododecane are conducted to evaluate the effect of organic modifiers on the viscoelastic properties of PCN. The mean value of storage modulus (E'), loss modulus (E''), and loss factor (tanδ) have been presented graphically in Figures 7–9, respectively. From these figures it is observed that all PCNs have higher storage modulus, loss modulus, and loss factor in comparison to pristine polymer. The PCN-lauric has the highest storage modulus, loss modulus, and loss factor followed by PCN-dodecyl and PCN-dodecane. Thus it is seen that the viscoelastic properties follow the same sequence of magnitude in PCNs as the elastic modulus. The stor-

TABLE VI
Elastic Modulus and Hardness of PA6 Based PCNs Containing Different Organic Modifiers

Sample (col. 1)	Elastic modulus E (GPa)	Hardness H (GPa)
PCN-lauric-9%	5.460 ± 0.267	0.170 ± 0.026
PCN-dodecyl-9%	4.766 ± 0.108	0.168 ± 0.008
PCN-dodecane-9%	4.417 ± 0.010	0.172 ± 0.013
Pure PA6	3.352 ± 0.169	0.121 ± 0.010

TABLE VII
Elastic Modulus and Hardness of PCN-Lauric for Different wt % of OMMT Loading

Sample (col. 1)	Elastic modulus E (GPa)	Hardness H (GPa)
PCN-lauric-9%	5.460 ± 0.267	0.170 ± 0.026
PCN-lauric-6%	4.748 ± 0.064	0.200 ± 0.001
PCN-lauric-3%	4.431 ± 0.044	0.194 ± 0.013
Pure PA6	3.352 ± 0.169	0.121 ± 0.010

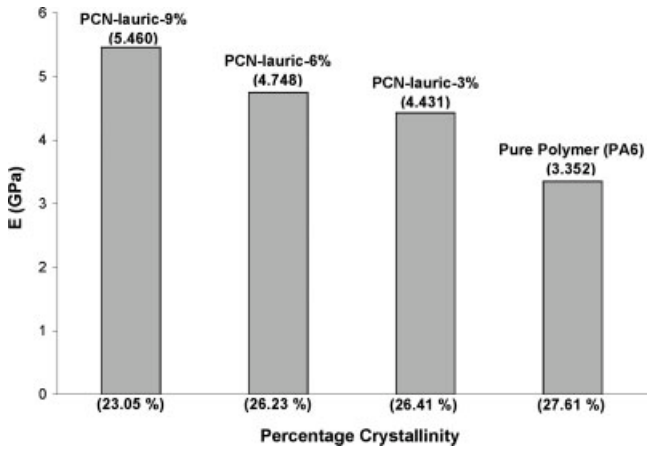

Figure 6 Effect of OMMT loading rate on elastic modulus of PCN-lauric.

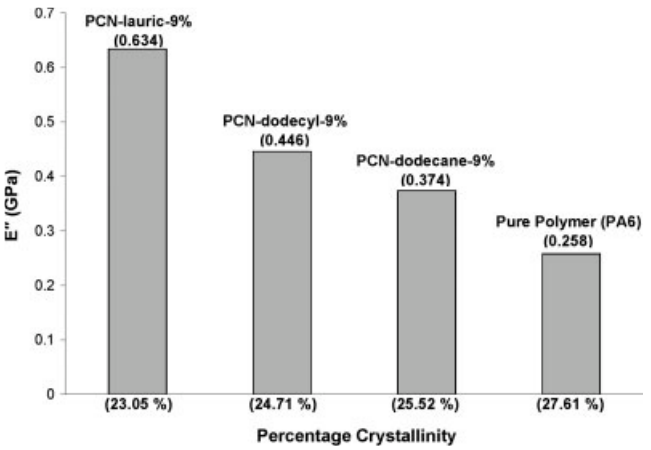

Figure 8 Effect of organic modifiers on loss modulus of PA6 based PCNs.

age and loss moduli in PCN-lauric are much higher than those of other two PCNs. However, the difference in magnitude of these moduli between PCN-dodecyl and PCN-dodecane are relatively less. The PCNs with same polymer and clay but with different organic modifiers exhibit different storage modulus, loss modulus, and loss factor. This clearly indicates that organic modifiers also influence the viscoelastic properties of PCN.

In dynamic mechanical testing using NanoDMA, a sinusoidal load is applied to the sample. The energy recovered and energy absorbed in response to the cyclic loading pattern is measured. The loss modulus gives the quantity of energy lost or absorbed by the material after withdrawal of load, which signifies the viscous property of the viscoelastic material. The storage modulus is the measure of energy recovered from cyclic loading and represents the elastic property of sample under cyclic loading. The ratio of loss and storage modulus is the loss factor, which represents the viscoelastic property of material.

The storage moduli of PCNs are found to be higher than that of pure polymer as shown in Figure 7. Again, PCNs with different organic modifiers give different storage modulus. In PCN, the clay nanofillers act as reinforcing agent. The reinforcing effect of nanoclay fillers may contribute towards the increase in storage modulus of PCN in comparison to pure polymer. The mechanical behavior of PCN is significantly influenced by the crystallinity of polymer and interfacial interactions of the constituents of PCN. The PCNs are synthesized with same polymer and clay, however, with different organic modifiers. The presence of different organic modifiers results in varying amounts of interactions in the PCNs, which are likely to produce different amounts of crystallinity in the PCNs. Thus variation in storage modulus in different PCNs may be attributed to the difference in crystallinity in PCNs.

Because of clay inclusions and interactions between constituents, the mobility of polymer chains in PCNs decreases in comparison to pristine polymer. It appears that in response to loading and unloading in

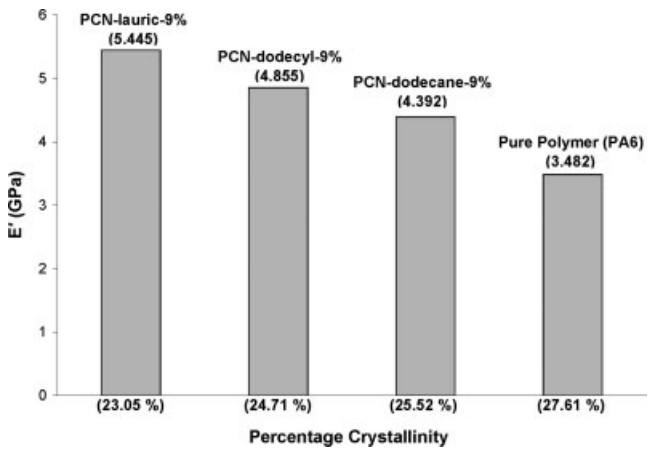

Figure 7 Effect of organic modifiers on storage modulus of PA6 based PCNs.

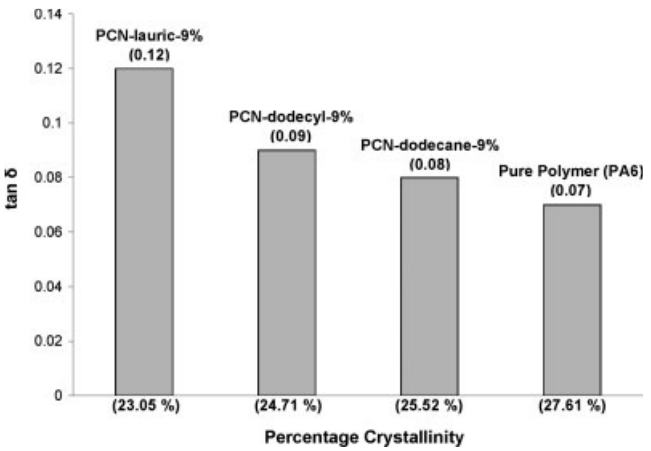

Figure 9 Effect of organic modifiers on loss factor of PA6 based PCNs.

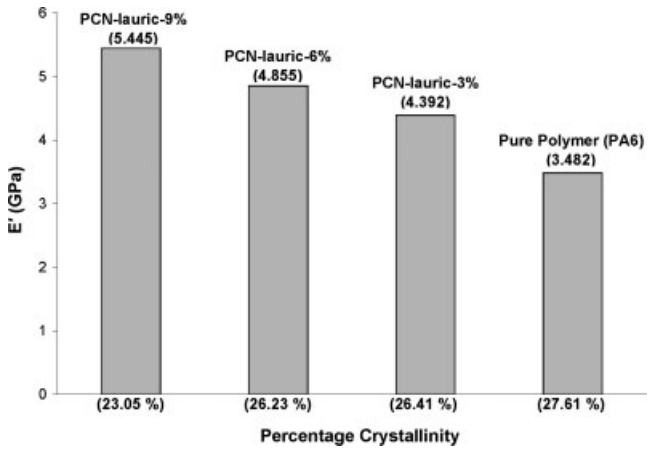

Figure 10 Effect of OMMT loading on storage modulus of PCN-lauric.

the dynamic mechanical test, the polymer chains take more time to rearrange themselves as compared to the pure polymer. This additional immobility of polymer in PCN may be attributed to the higher loss modulus of PCN in comparison to pure polymer.

In the presence of different organic modifiers, the crystallinity and hence interactions of polymer with clay and modifiers vary possibly resulting in the different hindrance to polymer mobility and consequently producing different loss modulus in PCNs containing different organic modifiers. It appears that crystallinity of intercalated polymer influences the interactions between polymer and clay, which in turn affects the mobility of polymer chains in PCN. The PCN-dodecane has least loss modulus between the PCNs. The other two PCNs have relatively higher loss modulus, which may indicate higher polymer chain immobility as a result of comparatively lesser crystallinity of polymer in PCNs.

The loss and storage modulus for the PCNs have same increasing or decreasing trends. It is observed that PCN-lauric shows higher loss modulus as well as storage modulus. Thus PCN-lauric shows higher elastic and viscous properties with respect to pure polymer than the other two PCNs. However, the values of PCN-lauric are not much higher than other two modifiers as seen in Figures 7–9, and PCN-dodecane and PCN-dodecyl have very close values of loss factor as evidenced from Figure 9.

Effect of clay loading on nanodynamic mechanical property of PCN

The results of viscoelastic properties of PCN-lauric with increased clay loading are graphically presented in Figures 10–12. As seen from these figures, with increasing clay loading, the loss factor, storage, and loss modulus increases in PCN-lauric. For increasing nanoclay fillers, the reinforcing effect of polymer increases and this produces higher storage modulus in PCN. As discussed previously in this paper, as the clay loading is increased, the crystallinity of the polymer decreases. The increased immobility of polymer chain may be attributed to the increase of loss modulus with the increase of clay loading rate. With the increase of clay loading in PCN-lauric, the loss and storage modulus are both found to increase considerably. However, as the loss and storage modulus increase or decrease, the loss factor which is the ratio of two moduli does not change by a significant amount. The PCN-lauric with 9% clay loading has distinctly higher value of loss factor than the other two PCNs. However, the PCNs with 6 and 3% clay loading have the same loss factor.

SUMMARY AND CONCLUSIONS

1. Dynamic nanoindentation experiments have been conducted for the first time to evaluate viscoelastic properties (storage modulus, loss

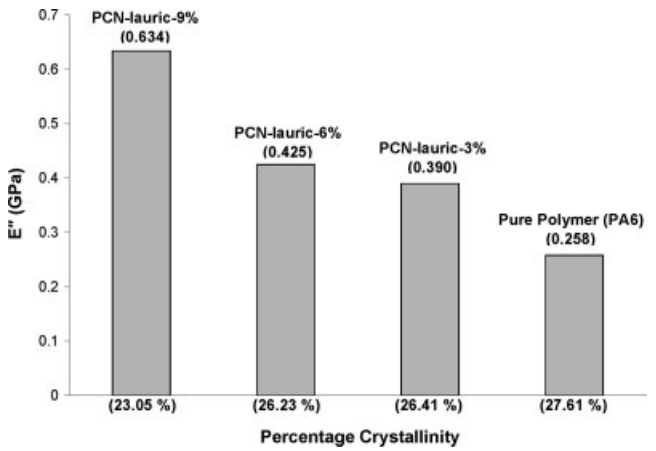

Figure 11 Effect of OMMT loading on loss modulus of PCN-lauric.

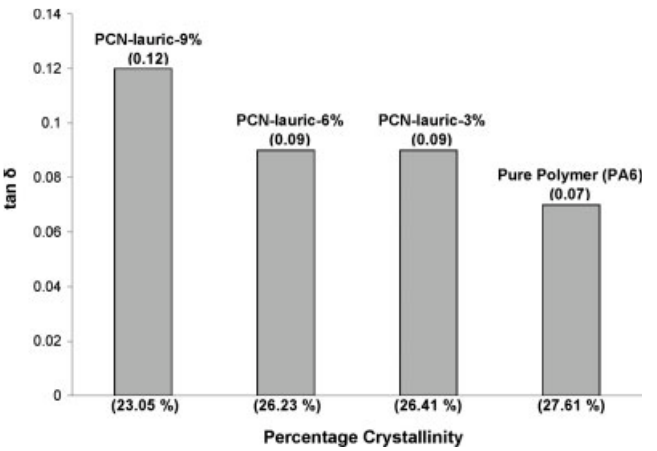

Figure 12 Effect of OMMT loading on loss factor of PCN-lauric.

modulus, and loss factor) of PCN. The PCNs show higher storage modulus, loss modulus, and loss factor in comparison to pure polymer.
2. PA6 based PCNs containing three different organic modifiers show different viscoelastic properties, indicating that organic modifiers influence the viscoelastic properties of PCNs. The viscoelastic (storage modulus, loss modulus, and loss factor) properties increase with increasing amount of clay loading in PCN.
3. The nanoindentation test results show that the PCNs containing three different organic modifiers show different elastic modulus, indicating that organic modifiers have significant influence on the elastic modulus of PCN. PCNs have higher elastic modulus and hardness in comparison to those of pure polymer.
4. In nanoindentation tests, PCNs show higher elastic modulus with increase in clay loading. The nanoclay fillers reduce crystallinity and also appear to act as reinforcing agent in PCN, resulting in higher magnitude of modulus.
5. From the DSC and XRD results, it is observed that PA6 based PCNs with different organic modifiers show different crystallinity, indicating that organic modifiers have influence on the crystallinity of PCNs. Pure polymer shows higher crystallinity in comparison to all the PCNs. Crystallinity of PCN reduces with increase of clay loading as observed in the case of PCN-lauric with different amount of clay loading.
6. The presence of different organic modifiers results in the different amount of crystallinity in the PCNs containing same polymer and clay. With decrease in percentage of crystallinity in the PCNs, the elastic modulus, storage modulus, loss modulus, and loss factor increases. It appears that interactions between the constituents of PCNs result in change in crystallinity, which in turn significantly affects the nanomechanical properties.

Authors acknowledge the support from National Science Foundation for purchase of atomic force microscopy and nanoindentation equipment used in this research. Authors would also acknowledge support from program manager Dr. Richard J. Fragaszy. The author DS acknowledges support from graduate school doctoral dissertation fellowship of North Dakota State University.

References

1. Okada, A.; Kawasumi, M.; Usuki, A.; Kojima, Y.; Kurauchi, T.; Kamigaito, O. Mater Res Soc Symp Proc 1990, 171, 45.
2. Pinnavaia, T. J.; Lan, T. Proc Am Soc Compos Tech Conf 1996, 11, 558.
3. Giannelis, E. P. Adv Mater 1996, 8, 29.
4. Maity, P.; Yamada, K.; Okamoto, M.; Ueda, K.; Okamoto, K. Chem Mater 2002, 14, 4656.
5. Pramanik, M.; Srivastava, S. K.; Biswas, K. S.; Bhowmick, A. K. J Appl Polym Sci 2003, 87, 2216.
6. Zhang, G.; Jiang, C.; Su, C.; Zhang, H. J Appl Polym Sci 2003, 89, 3155.
7. Wang, D.; Wilkie, C. A. Polym Degrad Stab 2003, 80, 171.
8. Lim, S. T.; Lee, C. H.; Choi, H. J.; Jhon, M. S. J Polym Sci Part B: Poly Phys 2003, 41, 2052.
9. Park, H. M.; Lee, W. K.; Park, C. Y.; Cho, W. J.; Ha, C. S. J Mater Sci 2003, 38, 909.
10. Chen, G. X.; Hao, G. J.; Guo, T. Y.; Song, M. D.; Zhang, B. H. J Mater Sci Lett 2002, 21, 1587.
11. Ma, C. C. M.; Kuo, C. T.; Kuan, H. C.; Chiang, C. L. J Appl Polym Sci 2003, 88, 1686.
12. Pramoda, K. P.; Liu, T.; Liu, Z.; He, C.; Sue, H. J. Polym Degrad Stab 2003, 81, 47.
13. Wang, S.; Hu, Y.; Wang, Z.; Yong, T.; Chen, Z.; Fan, W. Polym Degrad Stab 2003, 80, 157.
14. Zhang, J.; Wilkie, C. A. Polym Degrad Stab 2003, 80, 163.
15. Liu, T.; Lim, K. P.; Tjiu, W. C.; Pramoda, K. P.; Chen, Z. K. Polymer 2003, 44, 3529.
16. Kim, T. H.; Lim, S. T.; Lee, C. H.; Choi, H. J.; Jhon, M. S. J Appl Polym Sci 2003, 87, 2106.
17. Priya, L.; Jog, J. P. J Polym Sci Part B: Polym Phys 2003, 41, 31.
18. Krikorian, V.; Kurian, M.; Galvin, M. E.; Nowak, A. P.; Deming, T. J.; Pochan, D. J. J Polym Sci Part B: Polym Phys 2002, 40, 2579.
19. Xu, M.; Choi, Y. S.; Kim, Y. K.; Wang, K. H.; Chung, I. J Polym 2003, 44, 6387.
20. Tang, Y.; Hu, Y.; Song, L.; Zong, R.; Gui, Z.; Chen, Z.; Fan, W. Polym Degrad Stab 2003, 82, 127.
21. Chang, J. H.; Park, D. K. Polym Bull 2001, 47, 191.
22. Katti, K. S. Colloids Surf B 2004, 39, 133.
23. Schmidt, S. R.; Katti, D. R.; Ghosh, P.; Katti, K. S. Langmuir 2005, 21, 8069.
24. Katti, D. R.; Ghosh, P.; Schmidt, S. R.; Katti, K. S.; Biomacromolecules 2005, 6, 3276.
25. Tabor D. The Hardness of Metals; Oxford University Press: London, 1951.
26. Oliver, W. C.; Pharr, G. M. J Mater Res 1992, 7, 1564.
27. Pethica, J. B.; Oliver, W. C. Physica Scripta 1987, T19A, 61.
28. Asif, A. S. A.; Pethica, J. B. Mater Res Symp Proc 1998, 505, 103.
29. Shen, L.; Phang, I. Y.; Liu, T.; Zeng, K. Polymer 2004, 45, 3341.
30. Beake, B. D.; Chen, S.; Hull, J. B.; Gao, F. J Nanosci Nanotechnol 2002, 2, 73.
31. Shen, L.; Phang, I. Y.; Liu, T.; Zeng, K. Polymer 2004, 45, 8221.
32. Shen, L.; Tjiu, W. C.; Liu, T. Polymer 2005, 46, 11969.
33. Shen, L.; Phang, I. Y.; Liu, T. Polym Test 2006, 25, 249.
34. Hu, Y.; Shen, L.; Yang, H.; Wang, M.; Liu, T.; Liang, T. Polym Test 2006, 25, 492.
35. Nai, M. H.; Lim, C. T.; Zeng, K. Y.; Tan, V. B. C. J Metastable Nanocrystalline Mater 2005, 23, 363.
36. Beake, B. D.; Goodes, S. R. J Mater Res 2004, 19, 237.
37. Bhaskar, A.; Tortorella, N.; Zaman, A. A.; Beatty, C. L. Annual Technical Conference, Nashville, Tennessee, May 4–8, 2003; Vol. 3, p 3722.
38. Lee, J. W.; Kim, M. H.; Choi, W. M.; Park, O. O. J Appl Polym Phys 2006, 99, 1752.
39. Sengupta, R.; Bandopadhyay, A.; Sabharwal, S.; Chaki, T. K.; Bhowmik, A. K. Polymer 2005, 46, 3343.
40. Odegard, G. M.; Gates, T. S.; Herring, H. M. Exp Mech 2005, 45, 130.
41. Choi, J. S.; Lim, S. T.; Choi, H. J.; Pozsgay, A.; Sazazdi, L.; Pukanszky, B. J Mater Sci 2006, 41, 1843.
42. Yuan, M.; Turng, L. S. Polymer 2005, 46, 7273.

43. Gahleitner, M.; Kretzschmar, B.; Pospiech, D.; Ingolic, E.; Reichelt, N. J Appl Polym Sci 2006, 100, 183.
44. Sung, Y. T.; Kum, C. K.; Lee, H. S.; Kim, J. S.; Yoon, H. G.; Kim, W. N. Polymer 2006, 46, 11844.
45. Liu, X.; Wu, Q.; Berglund, L. A.; Lindberg, H.; Fan, J.; Qi, Z. J Appl Polym Sci 2003, 88, 953.
46. Garcia, M.; Tauriel, J. G.; Norder, B.; Francisco, C.; Kooi, B. J.; Zyl, W. E. V.; Verweij, H.; Blank, D. H. A. Adv Eng Mater 2004, 6, 724.
47. Lee, C. S.; Jho, J. Y.; Choi, K.; Hwang, T. W. Macromol Res 2004, 12, 141.
48. Xie, S.; Zhang, S.; Wang, F.; Liu, H.; Yang, M. Polym Eng Sci 2005, 45, 1247.
49. Pluta, M.; Paul, M. A.; Alexandre, M.; Dubois, P. J Polym Sci Part B: Polym Phys 2006, 44, 299.
50. Park, K.; Mishra, S.; Lewis, G.; Losby, J.; Fan, Z.; Park, J. B. Biomaterials 2004, 25, 2427.
51. Asif, S. A. S.; Wahl, K. J.; Colton, R. J.; Warren, O. L. J Appl Phys 2001, 90, 1192.
52. Hayes, S. A.; Goruppa, A. A.; Jones, F. R. J Mater Res 2004, 19(11), 3298.
53. Mohanty, B.; Katti, K. S.; Katti, D. R.; Verma, D. J Mater Res 2006, 21 2045.
54. Dencheva, N.; Nunes, T. G.; Oliviera, M. J.; Denchev, Z. J Polym Sci Part B: Polym Phys 2005, 43, 3720.
55. Jafari, S. H.; Gupta, A. K. J Appl Polym Sci 1999, 71, 1153.
56. Puiggali, J.; Franco, L.; Aleman, C.; Subirana, J. A. Macromolecules 1998, 31, 8540.
57. Liu, X.; Breen, C. Macromol Rapid Commun 2005, 26, 1081.
58. Wu, T. M.; Liao, C. S. Macromol Chem Phys 2000, 201, 2820.
59. Song, J. B.; Ren, M. Q.; Chen, Q. Y.; Wang, S. Y.; Zhao, Q. X.; Zhang, H. F.; Mo, Z. S. Chinese J Polym Sci 2004, 22, 491.
60. Hermans, P. H.; Weidinger, A. J Polym Sci 1949, IV, 709.
61. Ricou, P.; Pinel, E.; Juhasz, N. International Center for Diffraction Data, Adv X-ray Analys 2005, 48, 170.
62. Bunn, C. W. Mol. Behav Dev Polym Mater; Chapman and Hall: London, 1975; p 337.
63. Holmes, D. R.; Bunn, C. W.; Smith, D. J. J Polym Sci 1955, 17, 159.
64. Kinoshita, Y.; Makromolekulare Chemie 1959, 33, 21.
65. Ruland, W. Polymer 1964, 5, 89.
66. Hedicke, K.; Wittich, H.; Mehler, C.; Gruber, F.; Altstadt, V. Compos Sci Technol 2006, 66, 571.
67. Krishenbaum, I.; Thomas, R. M.; Kennedy, J. P.; J Polym Sci Part B: Polym Phys 1963, 1, 789.
68. Winberg, P.; Eldrup, M.; Pedersen, N. J.; Es, M. A. V.; Maurer, F. H. J Polym 2005, 46, 8239.
69. Lin, Y.; Zhong, W.; Shen, L.; Xu, P.; Du, Q. J Macromol Sci Part B: Polym Phys 2005, 44, 161.
70. Kojima, Y.; Matsuoka, T.; Takahashi, H.; Kurauchi, T. J Appl Polym Sci 1994, 51, 683.
71. Jiang, T.; Wang, Y.; Yeh, J.; Fan, Z. Eur Polym J 2005, 41, 459.
72. Li, Y.; Liu, H.; Zhang, Y.; Yang, G. J Appl Polym Sci 2005, 98, 2172.
73. Inan, G.; Celik, C.; Patra, P. K. Proceedings of the NATAS 31st Annual Conference on Thermal Analysis and Applications, 2003, 31, 1.
74. Gopakumar, T. G.; Lee, J. A.; Kontopoulou, M.; Parent, J. S. Polymer 2002, 43, 5483.
75. Meneghetti, P.; Qutubuddin, S. Thermochim Acta 2006, 442, 74.
76. Homminga, D. S.; Goderis, B.; Mathot, V. B. F.; Groeninckx, G. Polymer 2006, 47, 1630.
77. Katti, K. S.; Sikdar, D.; Katti, D. R.; Ghosh, P.; Verma, D. Polymer 2006, 47, 403.
78. Scott, W. W.; Bhushan, B. Ultramicroscopy 2003, 97, 151.
79. Hatakeyama, T.; Quinn, F. X. Thermal Analysis: Fundamentals and Applications to Polymer Science, 2nd ed.; Wiley: New York, 1999.
80. Zhang, T. Y.; Xu, W. H. J Mater Res 2002, 17, 1715.
81. Gurato, G.; Fichera, A.; Grandi, F. Z.; Zannetti, R.; Canal, P. Die Makromol 1974, 175, 953.
82. Vaia, R. A. In Polymer-Clay Nanocomposites; Pinnavaia, T. J.; Beall, G. W., Eds.; Wiley: New York, 2002; p 229.
83. Sikdar, D.; Katti, D. R.; Katti, K. S. Langmuir 2006, 22, 7738.
84. Sikdar, D.; Katti, D. R.; Katti, K. S.; Bhowmick, R. Polymer 2006, 47, 5196.